A&A 663, A42 (2022)
https://doi.org/10.1051/0004-6361/202243776

Astronomy & Astrophysics

Radial distribution of plasma at comet 67P

Implications for cometary flyby missions

N. J. T. Edberg[1], F. L. Johansson[1], A. I. Eriksson[1], E. Vigren[1], P. Henri[2,3], and J. De Keyser[4]

[1] Swedish Institute of Space Physics (IRF), Uppsala, Sweden
e-mail: ne@irfu.se
[2] Laboratoire de Physique et Chimie de l'Environnement et de l'Espace, CNRS, Orléans, France
[3] Laboratoire Lagrange, OCA, CNRS, UCA, Nice, France
[4] Royal Belgian Institute for Space Aeronomy, BIRA-IASB, Brussels, Belgium

Received 13 April 2022 / Accepted 31 May 2022

ABSTRACT

Context. The Rosetta spacecraft followed comet 67P/Churyumov-Gerasimenko (67P) for more than two years at a slow walking pace ($\sim$1 m s^{-1}) within 1500 km from the nucleus. During one of the radial movements of the spacecraft in the early phase of the mission, the radial distribution of the plasma density could be estimated, and the ionospheric density was found to be inversely proportional to the cometocentric distance r from the nucleus (a $1/r$ distribution).
Aims. This study aims to further characterise the radial distribution of plasma around 67P throughout the mission and to expand on the initial results. We also aim to investigate how a $1/r$ distribution would be observed during a flyby with a fast ($\sim$10's km s^{-1}) spacecraft, such as the upcoming Comet Interceptor mission, when there is also an asymmetry introduced to the outgassing over the comet surface.
Methods. To determine the radial distribution of the plasma, we used data from the Langmuir probe and Mutual Impedance instruments from the Rosetta Plasma Consortium during six intervals throughout the mission, for which the motion of Rosetta was approximately radial with respect to the comet. We then simulated what distribution a fast flyby mission would actually observe during its passage through a coma when there is a $1/r$ plasma density distribution as well as a sinusoidal variation with a phase angle (and then a sawtooth variation) multiplied to the outgassing rate.
Results. The plasma density around comet 67P is found to roughly follow a $1/r$ dependence, although significant deviations occur in some intervals. If we normalise all data to a common outgassing rate (or heliocentric distance) and combine the intervals to a radial range of 10–1500 km, we find a $1/r^{1.19}$ average distribution. The simulated observed density from a fast spacecraft flying through a coma with a $1/r$ distribution and an asymmetric outgassing can, in fact, appear anywhere in the range from a $1/r$ distribution to a $1/r^2$ distribution, or even slightly outside of this range.
Conclusions. The plasma density is distributed in such a way that it approximately decreases in a manner that is inversely proportional to the cometocentric distance. This is to be expected from the photoionisation of a collision-less, expanding neutral gas at a constant ionisation rate and expansion speed. The deviation from a pure $1/r$ distribution is in many cases caused by asymmetric outgassing over the surface, additional ionisation sources being present, electric fields accelerating plasma, and changing upstream solar wind conditions. A fast flyby mission can observe a radial distribution that deviates significantly from a $1/r$ trend if the outgassing is not symmetric over the surface. The altitude profile that will be observed depends very much on the level of outgassing asymmetry, the flyby velocity, the comet rotation rate, and the rotation phase. It is therefore essential to include data from both the inbound and outbound legs, as well as to compare plasma density to neutral density to get a more complete understanding of the radial distribution of the plasma.

Key words. plasmas – comets: general

1. Introduction

The Rosetta spacecraft followed comet 67P/Churyumov-Gerasimenko (hereafter 67P) from 2014 until 2016. During this time, 67P and Rosetta moved from a heliocentric distance of 3.6 AU to perihelion at 1.2 AU, and outwards again. Due to the very low gravity, Rosetta moved in non-Keplerian trajectories around the comet nucleus, from cometocentric distances of about 10 km to a maximum of 1500 km during one of the far excursions. Different regimes of the plasma environment could be sampled because the trajectory changed often. Some of these trajectories included a more rapid change in distance over time (albeit still at a walking pace of $\sim$1 m s^{-1}), such that the radial distribution of the plasma could be studied.

As the comet approached the Sun, the outgassing caused by the sublimation of volatile material increased rapidly (Hansen et al. 2016; Läuter et al. 2018). At Rosetta's arrival in 2014, the outgassing rate was of the order of 10^{25}–10^{26} s^{-1}, while at perihelion it reached a maximum of some 10^{28} s^{-1}. Negligible gravity means that the outgassing material can expand freely into space. Impinging solar radiation in the extreme ultra-violet (EUV) range subsequently ionises some of the neutral species such that an ionosphere is formed (Edberg et al. 2015; Vigren et al. 2015, 2016; Galand et al. 2016; Johansson et al. 2017). Additional ionisation is also caused by electron impacts at a rate which sometimes exceeds the photoionisation rate (Heritier et al. 2018). Charge exchange processes are also present and, while not being a net source of ions, they change the physico-chemistry

of the ionosphere (Simon Wedlund et al. 2020). The electron impact ionisation was more often the dominant ionisation source before March 2015 and after March 2016, in other words, beyond a heliocentric distance of about 2.5 AU, which corresponds to an outgassing rate of approximately 10^{26} s^{-1}. Electron impact ionisation can also significantly increase above the photoionisation rate during solar wind events, such as corotating interaction region (CIR) or coronal mass ejection (CME) impacts, when the flux of electrons increase (Edberg et al. 2016a,b; Hajra et al. 2018; Goetz et al. 2019).

The neutral density at a cometocentric distance r from a comet with a spherically symmetric outgassing rate Q can be approximated as

$$n_N \approx \frac{Q}{4\pi r^2 u_N}, \tag{1}$$

where u_N is the expansion velocity of the neutrals (Haser 1957). In this form, the exponential decay due to photo-dissociation and photoionisation is neglected, which is a reasonable assumption at distances within a few thousand kilometers of the nucleus (Vigren et al. 2015). We also need to assume that the sublimation of neutrals is homogeneous over the surface. In reality, this is often not the case and the density at a specific distance is the result of outgassing from different locations on the surface. This gives rise to fine-scale variations in the density, but the general trend of how the density varies with distance still holds as long as these fine-scale variations are generally smaller than the changes with distance. The ionospheric ion density can be expressed as

$$n_i = \nu n_N \frac{r - r_0}{u_i} \approx \frac{\nu Q}{4\pi r u^2}, \tag{2}$$

where ν is the total ionisation frequency, $r_0 (\ll r)$ is the radius of the comet, and u_i is the ion expansion velocity assumed constant and equal to the neutral velocity such that $u_n = u_i = u$. In this paper, we assume that the ion density is equal to the electron density, and no charged dust is present (Vigren et al. 2021, 2022). Further assumptions are needed to reach these expressions including equal ionisation frequency at all distances and stability on timescales of weeks. This is reasonable for photoionisation in an EUV transparent coma, but perhaps less so when electron impact ionisation becomes dominant and during rapid solar wind changes on timescales of hours (Vigren et al. 2015; Galand et al. 2016; Heritier et al. 2018).

We note that, according to Eqs. (1) and (2), the ionospheric density should fall off as $1/r$, while the neutral density should fall off as $1/r^2$. The $1/r$ distribution was experimentally confirmed using Rosetta measurements from when the spacecraft made an approximately radial movement from a few tens of kilometers out to 300 km (Edberg et al. 2015). Before Rosetta, measurements from the Giotto flyby of comet 1P/Halley, with an outgassing rate one to two orders of magnitude higher than that of 67P at comparable distances to the Sun, had shown that inside the so-called contact surface, the density indeed falls off as $1/r$. Outside of this boundary, the plasma density instead appeared to fall off as $1/r^2$. As the plasma velocity showed a linear increase with cometocentric distance (rather than a constant speed as was the case closer to the nucleus for Rosetta at 67P), this led to the plasma density falling off as $1/r^2$ (Balsiger et al. 1986). The change in distribution at the contact surface was explained as a change in the electron temperature, which would cause a significant change in the electron recombination rate (Altwegg et al. 1993). This was also corroborated by simulations with a good data-model agreement (Rubin et al. 2014). The neutral density showed the same slope ($1/r^2$) during the entire encounter, while dust measurements indicated a local peak at roughly the same cometocentric distance as the distance of the transition from $1/r$ to $1/r^2$ (Levasseur-Regourd et al. 1999).

2. Datasets and instrumentation

In this paper we use ionospheric density measurements from the LAngmuir Probe (LAP) and the Mutual Impedance Probe (MIP) instruments of the Rosetta Plasma Consortium (RPC) (Eriksson et al. 2007; Trotignon et al. 2007; Carr et al. 2007) and neutral density data from the COmet Pressure Sensor (COPS) of the Rosetta Orbiter Spectrometer for Ion and Neutral Analysis (ROSINA) instrument (Balsiger et al. 2007), all taken from the Rosetta spacecraft (Glassmeier et al. 2007). LAP is a dual-Langmuir probe instrument comprised of two TiN-coated spheres mounted on two booms. The potentials of the probes are controlled such that they sweep from a maximum of −32V to +32V and measure the current from attracted or repelled ambient ions and electrons. From the characteristics of the resulting current-voltage curve, plasma properties such as density can be obtained. The MIP instrument measures the electric coupling in the plasma between an emitting and a receiving antenna in a frequency range that normally contains the plasma frequency line. The plasma density can thus be obtained, too, in an independent manner. The ionospheric density used in this paper was obtained from the slope of the positive voltage side of the RPC-LAP sweep when assuming a fixed electron temperature of 5 eV (a reasonable assumption for the intervals used in this paper; Eriksson et al. 2017), which was then cross-calibrated with RPC-MIP derived densities as described by Johansson et al. (2021) and referred to as 'NED' in the ESA PSA archive (Eriksson et al. 2020). The time resolution varied throughout the mission but was typically of the order of minutes. The neutral density time resolution was one min. For a more thorough explanation of the data, we refer readers to the instrument papers mentioned above.

3. Radial distribution of plasma at 67P

Figure 1 highlights six intervals throughout the mission when Rosetta made large radial movements relative to the comet nucleus. During the Rosetta mission, there were no dedicated campaigns for studies of the radial distribution of plasma, so for this study we can only use intervals when Rosetta, for varying reasons, moved significantly radially. We focus on intervals during which such significant radial variations were performed on limited time intervals in order to ensure that the comet was at a similar heliocentric distance. We can therefore assume that the solar illumination rate, which drives the cometary outgassing, was constant during each single interval. This means that both the radial distances and the duration of these movements were different in each of the six cases.

The chosen intervals lasted from about a week to several weeks and the radial changes were of the order of hundreds of kilometers to 1000 km. Interval 1 is included in a set of 'pyramid orbits' when Rosetta made an early mapping of the comet. Interval 2 occurred after a safe mode when the dust flux became too high and Rosetta quickly had to move to higher altitudes where the dust flux was lower, and subsequently back to somewhat lower altitudes again. Interval 3 was a transition from close orbits to orbits farther out. The same applies to interval 4, but it was

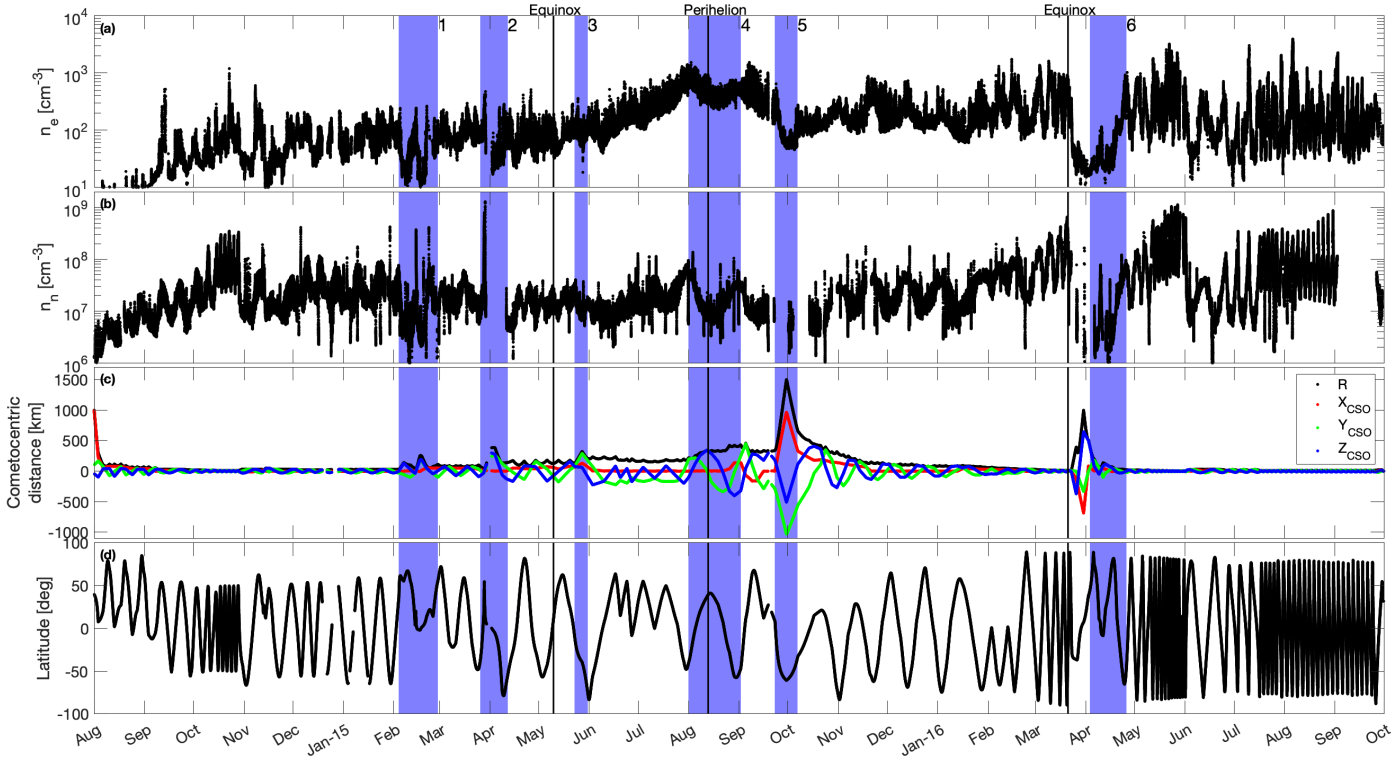

Fig. 1. Time series of Rosetta data from the arrival at comet 67P in 2014 until the end of the mission in 2016. *Panels a*: electron density, *b*: neutral density, *c*: cometocentric distance r and position components in the Cometocentric Solar Orbital (CSO) reference frame, and *d*: the latitude of Rosetta. In the CSO system, the x axis points towards the Sun, the z axis is directed out of the orbital plane of the comet, and the y axis completes the right-handed system. The blue vertical regions mark intervals when Rosetta performed approximately radial movements relative to the comet such that altitude profiles of the density could be obtained.

more stretched out in time and a more gradual radial movement occurred. Interval 5 is known as the dayside excursion which was intended to take Rosetta to the bow shock (at the time believed to be at a distance of 1500 km). Interval 6 is from the end of the night-side excursion. As the nightside of the comet is not illuminated and since the sublimation and the resulting outgassing change compared to the dayside, any comparison between nightside and dayside data becomes difficult. Therefore, in interval 6, we only include the end of the nightside excursion when Rosetta was back on the dayside again.

During all of these intervals, Rosetta continuously measured the electron density with the MIP and LAP instruments. The neutral density, from ROSINA/COPS, was normally measured continuously throughout the mission, but not so during intervals 2, 5, and 6. In these intervals, the neutral density measurements ceased either due to the safe-mode forcing the instrument to shut down, or due to the signal not reaching above the instrument detection limit.

Figure 2 shows the radial profiles of the electron density from each of the intervals mentioned together with the neutral density profiles (scaled by a factor of 10^5 to fit the plot). Fits were performed to both the electron density and the neutral density, and the resulting curves are shown as red and black lines together with the data. The fits were done to the median values of the data in 10 km bins to avoid any uneven sampling biases. The slope of each fit, that is, the electron density and neutral density dependence on radial distance, is indicated in each panel. There is considerable scatter in the data of the order of one magnitude in some cases. This is due to several factors including the following: that the activity of the point on the 67P surface from which the gas currently immersing Rosetta was emitted varies with geographic location and illumination at the local time, the solar wind conditions (e.g. dynamic pressure and convective electric field) change during these long intervals, the photo-ionisation rate changes with the solar variations, and the particle impact ionisation rate changes with ambient plasma conditions. Despite these factors, there is a clear tendency for the plasma density to fall off approximately as $1/r$, although with deviations. The 95% confidence intervals of the fit parameters are shown within the brackets next to the fit coefficients in each panel. A deviation is especially clear in interval 3, where the exponent is 0.5 rather than 1. An explanation for such a deviation could be that the distance and latitude were changing in phase with each other, such that the variation caused by changing the radial distance was counteracted by the turning of the nucleus under Rosetta. This could have caused neutral gas from a set of more active regions and/or from a larger illuminated area to be responsible for the outgassing in the Rosetta direction. The radial profiles of the neutral density do not follow the expected $1/r^2$ distribution in most intervals, which is most likely due to the asymmetric outgassing as well as Rosetta moving both radially and changing latitude and longitude at the same time.

To obtain a radial distribution that covers the entire range of the ionosphere of 67P, and also to increase the statistical accuracy of the radial distribution function, it would be desirable to combine these six intervals. However, as these intervals occurred at different heliospheric distances, and therefore during different levels of neutral outgassing rates (mainly depending on the solar illumination), any direct comparison between the intervals is not straightforward. Assuming that photoionisation is the main ionisation source, one could normalise the plasma density in each interval by dividing the plasma density by the neutral density.

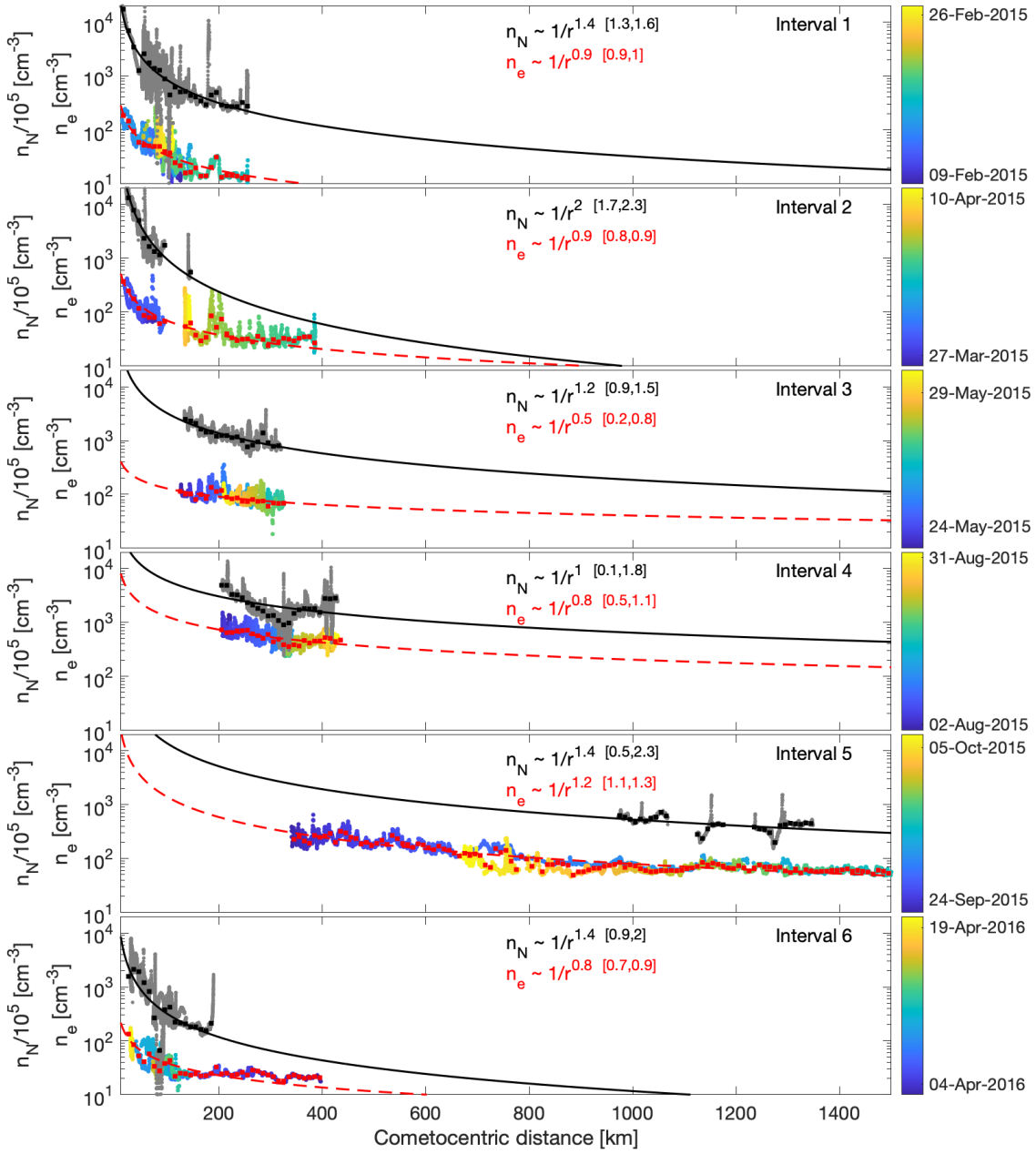

Fig. 2. Radial profiles of the electron density and neutral density during the six intervals indicated in Fig. 1. The neutral density was scaled by a factor 10^5 to fit the plot. The electron density data points are colour-coded by time. Fits were performed to the density profiles indicating how the density falls off with cometocentric distance. The fit parameters are shown in each panel together with the values in 95% confidence intervals.

However, since the neutral measurements only occured intermittently during three of the intervals, this is not always possible. Instead, we can use a model which describes the outgassing rate dependency on heliocentric distance. Hansen et al. (2016) showed that the outgassing rate of water $Q = c_1 R_h^{c_2}$, where R_h is the heliocentric distance, and c_1 and c_2 are constants determined from the fitting of ROSINA/COPS data. The fit changed from the inbound to the outbound leg of 67P's perihelion pass such that during the inbound leg $c_1 = 2.58 \times 10^{28}$ and $c_2 = -5.10$, while during the outbound leg $c_1 = 1.58 \times 10^{29}$ and $c_2 = -7.15$. We can use this expression to normalise the plasma density data to the conditions at perihelion, that is, an outgassing rate of $Q_{\max} = 10^{28}$ s^{-1}. One complication is that the model of Hansen et al. (2016) is only applicable to water, and water is not always the dominant species in the coma. Especially during interval 6, CO_2 was equally as abundant as water, while during the other intervals water was in fact dominant (Läuter et al. 2018). We therefore exclude interval 6 in the analysis below. Applying that simple normalisation procedure to intervals 1–5, and combining the intervals into one single dataset, we obtain a radial distribution spanning the interval 10–1500 km, as shown in Fig. 3. A fit was done to this dataset, to median values in 30 km bins, which indicates that the plasma density falls off as $\sim 1/r^{1.19}$.

This slope is somewhat steeper than the theoretically predicted inversely linear dependence. Reasons for that could again be that electron impact ionisation dominates in some intervals, and more so closer to the surface, that some geographic locations have a higher outgassing rate, that the possibility of non-radial plasma flows or that the change in the outgassing rate with heliocentric distance is not perfectly modelled. Imperfections of

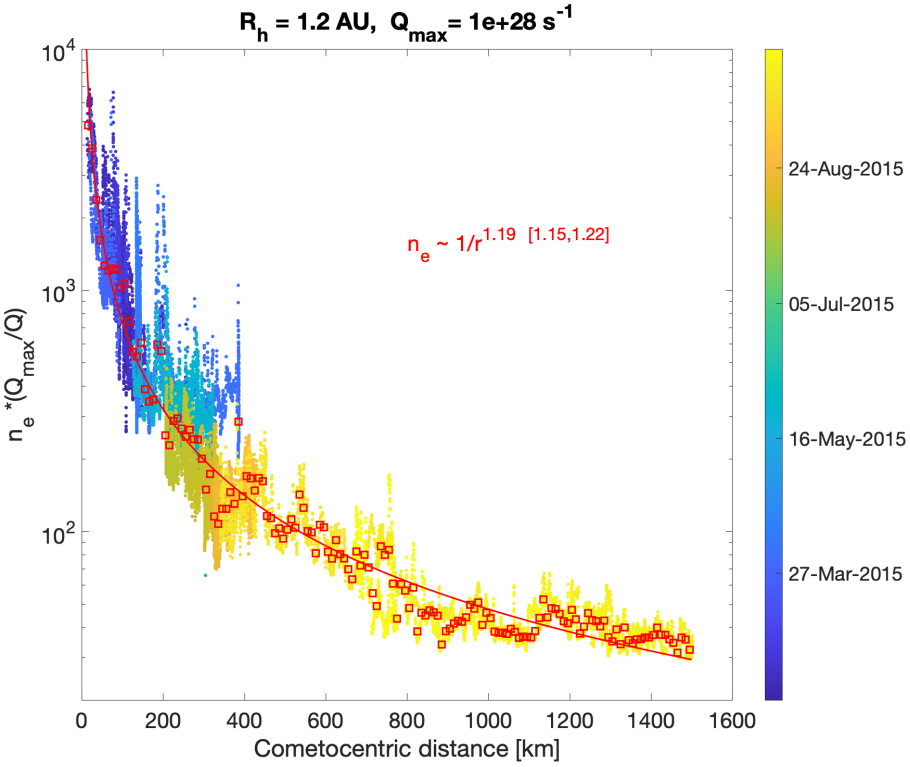

Fig. 3. Data from the six intervals in Fig. 1 combined into one plot. The electron density from each interval has been normalised to the outgassing rate of perihelion by using the outgassing rate model of Hansen et al. (2016) to obtain a single radial profile from approximately 10 to 1500 km. The data points are again colour-coded by time. A fit (red line) was performed to the data after it was binned in 10 km bins and median values were calculated (red squares). The exponent parameter of the fit and its 95% confidence interval is indicated in the figure.

the normalisation procedure can of course also play a part. For instance, raising the density during the dayside excursion (interval 5) by a factor of two would lead to an almost exact $1/r$ fit to the combined data.

4. Implications for fast flyby missions

In the previous section, we showed that the electron density on average falls off approximately as $1/r$, but with significant deviations due to varying outgassing rates over the surface of the comet in particular. As a next step, we are interested in how such a radial distribution of the plasma would be perceived if a spacecraft flew through the coma at high speeds, rather than at a walking pace similar to Rosetta. This question is motivated by the fact that flyby measurements have been performed in the past (e.g. Giotto, Vega 1, Vega 2, ICE etc.), and are also planned for the future (e.g. ESA's Comet Interceptor to be launched in 2029 with the objective to fly by a dynamically new comet), and it is not obvious that a comet with asymmetric outgassing would yield a simple $1/r$ radial profile in the measurements.

4.1. The case of asymmetric outgassing

In Fig. 4, we show what ionospheric density a spacecraft would observe during a flyby of a comet with an outgassing rate of 5×10^{29} s^{-1} (i.e. about the activity of comet 1P/Halley at perihelion), with a closest approach of 1000 km at the sub-solar point in the ecliptic plane and with a flyby speed of 40 km s^{-1}. We show this for three different outgassing cases: symmetric outgassing, an outgassing varying sinusoidally with phase angle, and an outgassing varying sawtooth-like with phase angle. Phase angle is defined here as the angle of rotation of the comet counted from the $+x_{CSO}$ axis in the clockwise direction.

Figure 4a shows the altitude of a simulated spacecraft flyby as a function of time. Using Eq. (2), we calculated the ionospheric density along the spacecraft track and plotted this in Fig. 4b. The plasma density thus falls off as $1/r$ exactly, which is reasonable in the inner part of the coma. We also assume a constant value of the solar wind density of 5 cm^{-3}, which was added to the cometary plasma density. At the closest approach, the plasma density reaches about 4000 cm^{-3}, and at a distance of 10^5 km, it drops to some 40 cm^{-3}. Figure 4b displays what would be measured in the simplest case of such a flyby where we neglect any effects of the solar wind-comet interaction, any electric field perturbations, chemistry, etc. as we are more interested in understanding the more basic effect that any asymmetric outgassing could have on the flyby measurements.

In the following step, we applied two different types of asymmetric outgassing profiles: in Fig. 4c a sinusoidal variation was multiplied to the ionospheric density and in Fig. 4e a sawtooth variation was multiplied to the ionospheric density. The form of these variations was chosen such that the ionospheric density would vary about an order of magnitude over one comet rotation. These variations represent a comet nucleus that rotates with a period of 2 days (similar to that of comet 1P/Halley), and whose surface properties vary significantly with the geographic location on the comet. The motivation for choosing such variations is that Rosetta observed similar variations around comet 67P. Sometimes there was a rather smooth, sinusoidal variation with the phase angle, and sometimes a more sawtooth-like variation was seen. The ionospheric density is still assumed to fall off inversely with the cometocentric distance. At some distance in the range 10^5–10^6 km, the density falls below 5 cm^{-3} and the solar wind density becomes dominant. In Figs. 4d,f, the corresponding along-track observations are shown. One can immediately see that the previously smooth and symmetric inbound and outbound density profiles are now quite disturbed. As the spacecraft approaches the comet, one side of the nucleus is facing the spacecraft. The nucleus rotates as the spacecraft flies past, but not with the same angular velocity as the phase angle of the spacecraft. Therefore, when the spacecraft is leaving the comet, another side

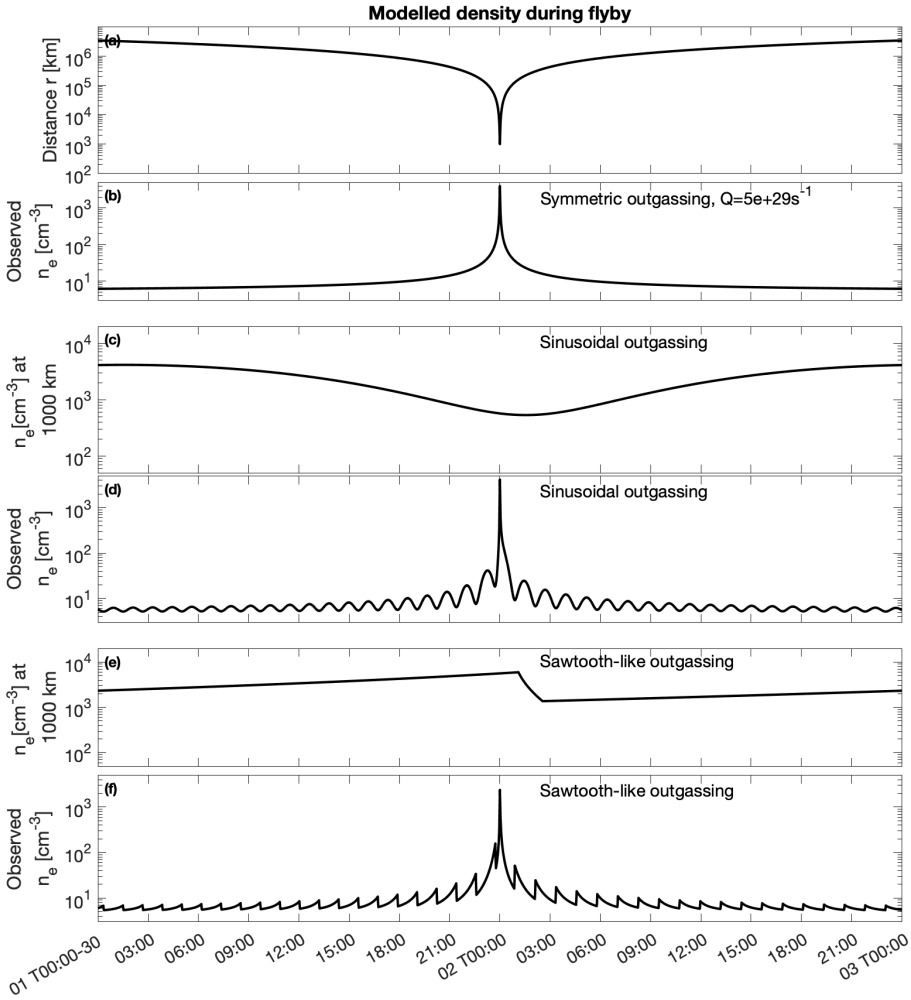

Fig. 4. Time series of (*a*): simulated cometocentric distance of a spacecraft flying past a comet at 40 km s^{-1} with a closest approach of 1000 km, (*b*): observed ionospheric density along this track, if assuming symmetric outgassing and a $1/r$ distribution, (*c*): density at a fixed point at R = 1000 km if a sinusoidally varying outgassing is introduced due to a rotating in-homogeneous nucleus, (*d*): along-track observed ionospheric density for a sinusoidally varying outgassing, (*e*): density at a fixed point at R = 1000 km if a sawtooth-like varying outgassing is introduced, (*f*): along-track density for the sawtooth variation in outgassing.

of the nucleus (with different outgassing) is underneath it and a different radial profile is observed.

We note that the rotating comet together with varying outgassing (with velocity u_i) give rise to a spiralling pattern of the gas surrounding the comet. Figure 5 shows, in a schematic way, what a spacecraft (S/C) would encounter during a flyby of such a rotating comet. As the S/C flies through this at a high speed, it will observe a 'Doppler-shifted' signal at a frequency of about $v_{S/C}/u_i$ = 40/1 higher than the comet rotation frequency. This can be seen in Figs. 4d,e where there is a 1.2 h periodicity rather than the 2 day periodicity from the comet rotation, as in Figs. 4c,e. There is also a different density profile on the inbound compared to the outbound leg.

A main point of this paper is that these profiles exhibit some structures that are not easily interpreted, at least not from the density record alone without other supporting data. In Fig. 6 we show the observed inbound and outbound altitude density profiles from the case of a sinusoidally varying plasma density (Fig. 4c), together with a $1/r$-distribution for comparison during the innermost part of the plasma environment ($<4 \times 10^4$ km).

The phase of the comet rotation is in this particular case 80°. In other words, the maximum outgassing is directed almost perpendicularly to the sun-comet line at the start of the flyby simulation. The outbound profile follows a $1/r$-distribution more closely than the inbound profile does, which falls off more rapidly with distance. The assumed rotation rate and its phase during the flyby play a large role in shaping the observed profiles. Therefore, in Fig. 7 we show the radial profiles for a range

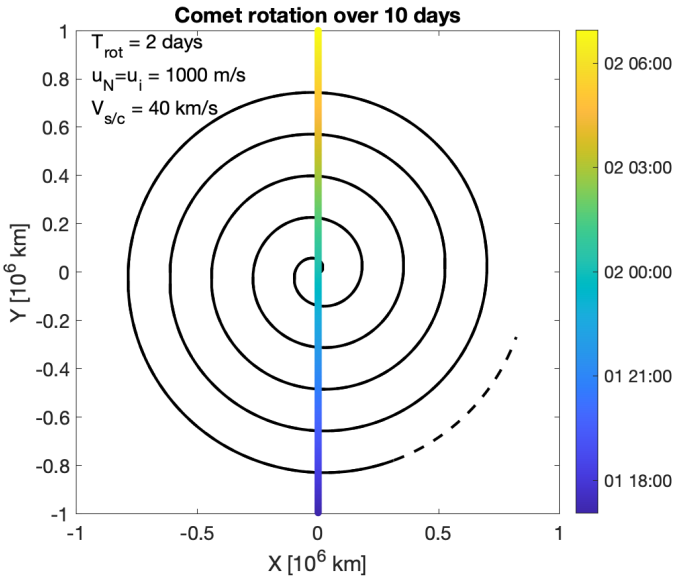

Fig. 5. Schematic illustration of a flyby through a coma where the comet is rotating with a period of 2 days and the outgassing is not constant over the surface. The black spiral indicates the maximum density, i.e. a phase-front, of the cometary plasma formed as the comet is outgassing (with a neutral and plasma velocity of 1 km s^{-1}) and rotating. The spiralling pattern is shown for 10 days of rotation, and will at some distance be smeared out by solar wind variations. The spacecraft is assumed to pass by at 40 km s^{-1} and takes about 12 h to cross this shown area.

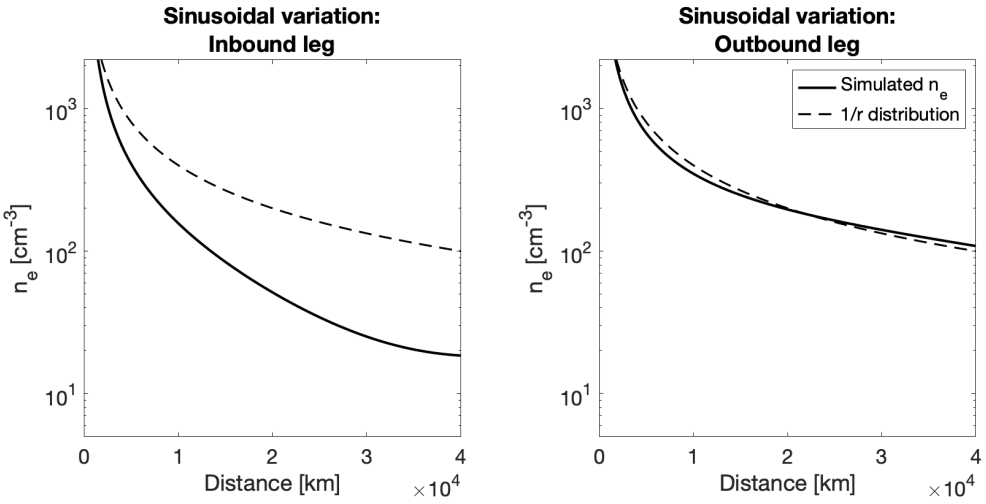

Fig. 6. The along-track observed ionospheric density for the case of a sinusoidally varying outgassing rate. A $1/r$-distribution is included for comparison (dashed line). Note the significant difference between the profiles on the inbound and the outbound leg.

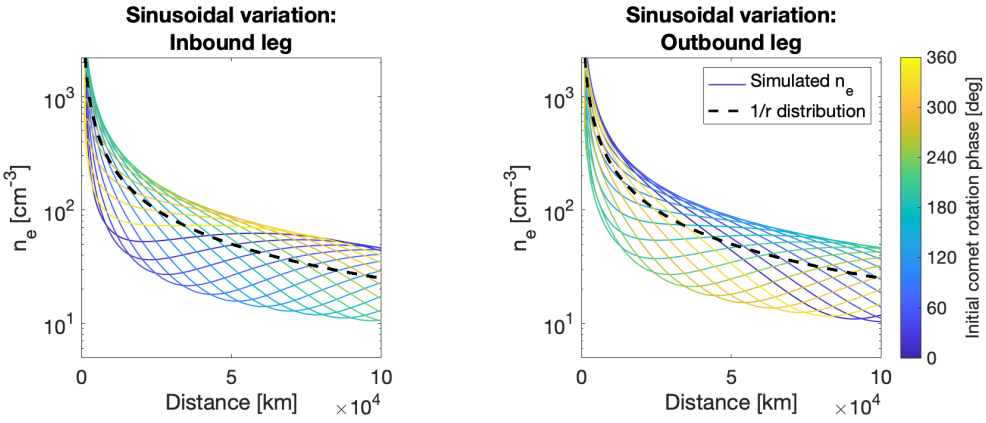

Fig. 7. Same as Fig. 6 but for a range of comet rotation phase angles from 0–360° in 10° steps, and ranging in distance out to 10^5 km.

of comet rotation phase angles out to 10^5 km. As can be seen, the radial profiles can take quite a large variety of shapes and several parameters contribute to shaping them. For instance, increasing the outgassing rate or decreasing the flyby closest approach distance would move these curves upwards (to a higher density). Increasing the rotation rate of the comet nucleus or the flyby speed would cause faster oscillations.

4.2. Transition from a 1/r to a 1/r² distribution

Figure 8 shows the inbound altitude profile from the case of the sawtooth varying outgassing. This is particularly interesting as the observed profile changes from an apparent $1/r^2$ distribution to an $1/r$ distribution even though the density is always modelled to drop off as $1/r$. The outgassing asymmetry, with the change across the sawtooth ledge, obviously changes the profile. The exact profile is again very dependent on the rotation rate of the comet, the rotation phase at the time of the flyby, the speed of the spacecraft, as well as the assumed variation in the outgassing (i.e. the shape of the sawtooth). Nevertheless, this particular case highlights the fact that the radial distribution of plasma can easily be misinterpreted from plasma density measurements alone, and such sharp changes as shown in Fig. 8 can be mistaken for a proper plasma boundary caused by a plasma process, rather than outgassing rate variations.

During the Giotto flyby of comet 1P/Halley, such a transition from a $1/r$ to a $1/r^2$ was observed, and the profile shown in Fig. 4 in Balsiger et al. (1986) is strikingly similar to the profile presented here. However, as the neutral gas measurement showed no such variation at 1P/Halley, the interpretation that the transition is due to a change in electron temperature and an associated change in the recombination rate is a more likely explanation. The neutral density measurements are therefore a great help in interpreting signatures in plasma density measurements. Correctly interpreting signatures in altitude profiles is also aided by the fact that inbound and outbound profiles are most likely very different from each other in the case of asymmetric outgassing.

5. Discussion

We have studied the radial distribution of plasma from measurements by Rosetta at comet 67P during six intervals in the mission. The plasma density, as measured by RPC MIP and LAP, show that the density does not always fall off exactly as the theoretically predicted $1/r$ distribution, but it is most often rather close to following this trend. Deviations are due to a number of reasons which include an uneven outgassing from the nucleus that rotates underneath Rosetta; changing levels of electron impact ionisation rates which also vary with cometocentric distance; solar wind velocity, density, magnetic field, and electric field changes; and changes to the photoionisation rate due to changing solar conditions during the longer-studied intervals. A combined plot from these intervals, where we have scaled the data to a common outgassing rate, reveals an overall $1/r^{1.19}$ radial density distribution.

As a next step, we investigate what radial distribution would be observed if measurements were taken by a fast flyby mission instead, similar to that of, for example, Giotto at comet 1P/Halley or the upcoming Comet Interceptor mission. Assuming a $1/r$-distribution and purely symmetric outgassing,

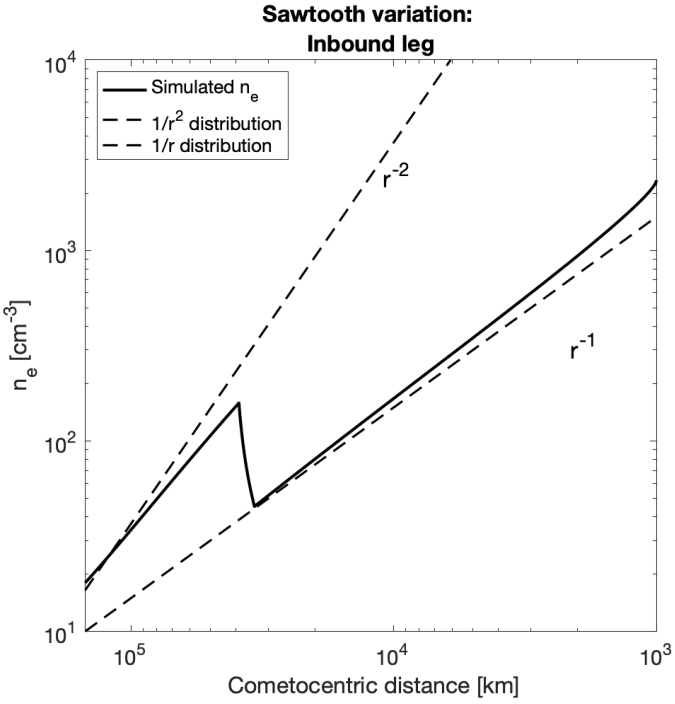

Fig. 8. Altitude density profile for the inbound leg of the sawtooth varying outgassing. Note the change from an apparent $1/r^2$ distribution to a $1/r$ distribution as the outgassing changes.

nothing unexpected would be observed. When introducing asymmetric outgassing, however, the situation becomes more complicated. We looked at two simple (and somewhat arbitrarily chosen) cases of a sinusoidally varying outgassing rate and a sawtooth-like outgassing pattern, intended to mimic the case of when the nucleus outgasses asymmetrically across its surface while the nucleus rotates at the same time.

The first case mainly results in the outbound and inbound density profiles looking quite different from each other with different slopes to the density-distance relation. Both steeper and less steep distributions compared to $1/r$ can appear. The exact shape very much depends on the rotation rate, the flyby speed, the phase of the rotation, and the assumed sinusoidal shape (including the magnitude of variation) of the outgassing rate.

This becomes even clearer when looking at the along-track density from the case of the sawtooth outgassing. Here, the apparent distribution can easily change from $1/r$ to $1/r^2$ at different cometocentric distances. The underlying $1/r$ distribution can appear steeper if the phase of the rotation is changing at the same time as the spacecraft is approaching the comet. A sharp ledge can be observed and easily mistaken for a plasma boundary when the crossing of the sawtooth occurs. It is quite striking that such a simple outgassing profile can give rise to a radial profile very similar to what was observed by Giotto at 1P/Halley. We have only modelled diurnal variations in the outgassing rate, while there could also be temporal changes due to jets or other sporadically occurring increases in the outgassing rate (Grün et al. 2016; Hajra et al. 2017), which could lead to similar alterations in the radial profiles.

The modelled $1/r$ distribution is most likely valid in the inner coma of a comet as was the case at 67P and also at 1P/Halley. However, farther out from the nucleus, this distribution can transition naturally to a steeper distribution regardless of any outgassing profile. Farther out, collisions become less frequent, acceleration by the solar wind convective electric field becomes more efficient, and recombination rates go down. Exactly where and for how long this transition to a steeper distribution occurs is uncertain and depends on several factors, but Giotto measurements at 1P/Halley observed such a transition (from $1/r$ to $1/r^2$) at about 2×10^4 km. In our model here we have assumed that there is no increase in velocity with radial distance to the comet. At 1P/Halley, Giotto observed a constant ion acceleration from about 2×10^4 km out to 10^5 km and a similar trend was found in the tail of 67P, while the dayside of 67P was more complicated as the ion flow direction was often against the direction of the Sun (Behar et al. 2018; Nilsson et al. 2020). The two comets were of course significantly different in terms of outgassing rates. Rosetta only measured out to about 10^3 km, and there was never any $1/r^2$ trend observed in the cold plasma. If our modelled $1/r$ distribution would instead naturally transition to a $1/r^2$ distribution farther out (in the range 10^3–10^5 km) without introducing an asymmetry to the outflow, it could be difficult to distinguish the effect that arises when the asymmetric outgassing is included.

6. Conclusions

We find that the ionospheric plasma within 1500 km around comet 67P on average falls off as $1/r^{1.19}$, although deviations do occur from this general trend. This is in approximate agreement with the theoretically assumed $1/r$ distribution. Any deviation is likely due to an uneven outgassing from the surface, varying levels of electron impact ionisation, imperfections of our model-based normalisation, and/or variations of solar wind conditions and local electric fields.

When using a $1/r$ distribution, but also applying an asymmetry to the outgassing, to model what a S/C would observe during a flyby mission through the inner coma, we find that the observed along-track altitude density profile can deviate significantly from a $1/r$ trend. Depending on the imposed asymmetry, the profile can appear as a $1/r^2$ distribution, or even shallower than a $1/r$ trend. A non-smooth outgassing profile can give rise to density-altitude profiles with sharp transitions that can easily be mistaken for plasma boundaries. If applying a convective electric field in the density model, asymmetries also arise in the along-track profiles due to this, which would complicate the situation further.

To be able to fully interpret plasma measurements correctly from a flyby mission, we must have knowledge of the underlying neutral gas density, and preferably the rotation rate of the comet. Other plasma properties, such as the distribution of higher energy ions and electrons as well as the magnetic field, will also help to disentangle variations due to other sources. The interpretation of the measurements in the comet plasma environment would also benefit greatly from having multi-point measurements, as this would help in disentangling spatial from temporal changes.

Acknowledgements. Rosetta is a European Space Agency (ESA) mission with contributions from its member states and the National Aeronautics and Space Administration (NASA). The work on RPC-LAP data was funded by the Swedish National Space Agency (SNSA). The work on RPC-MIP data was funded by CNES. The data used in this paper are available in the ESA PSA archive: http://archives.esac.esa.int/psa/ftp/INTERNATIONAL-ROSETTA-MISSION/ (Eriksson et al. 2020).

References

Altwegg, K., Balsiger, H., Geiss, J., et al. 1993, A&A, 279, 260
Balsiger, H., Altwegg, K., Buhler, F., et al. 1986, Nature, 321, 330

Balsiger, H., Altwegg, K., Bochsler, P., et al. 2007, Space Sci. Rev., 128, 745
Behar, E., Nilsson, H., Henri, P., et al. 2018, A&A, 616, A21
Carr, C., Cupido, E., Lee, C. G. Y., et al. 2007, Space Sci. Rev., 128, 629
Edberg, N. J. T., Eriksson, A. I., Odelstad, E., et al. 2015, Geophys. Res. Lett., 42, 2015GL064233
Edberg, N. J. T., Alho, M., André, M., et al. 2016a, MNRAS, 462, S45
Edberg, N. J. T., Eriksson, A. I., Odelstad, E., et al. 2016b, J. Geophys. Res. Space Phys., 121, 949
Eriksson, A. I., Boström, R., Gill, R., et al. 2007, Space Sci. Rev., 128, 729
Eriksson, A. I., Engelhardt, I. A. D., André, M., et al. 2017, A&A, 605, A15
Eriksson, A. I., Gill, R., Johansson, E. P. G., & Johansson, F. L. 2020, ESA Planetary Science Archive and Nasa Planetary Data System, Rosetta RPC-LAP archive of derived plasma parameters from the ROSETTA mission
Galand, M., Héritier, K. L., Odelstad, E., et al. 2016, MNRAS, 462, S331
Glassmeier, K.-H., Boehnhardt, H., Koschny, D., Kührt, E., & Richter, I. 2007, Space Sci. Rev., 128, 1
Goetz, C., Tsurutani, B. T., Henri, P., et al. 2019, A&A, 630, A38
Grün, E., Agarwal, J., Altobelli, N., et al. 2016, MNRAS, 462, S220
Hajra, R., Henri, P., Vallières, X., et al. 2017, A&A, 607, A34
Hajra, R., Henri, P., Myllys, M., et al. 2018, MNRAS, 480, 4544
Hansen, K. C., Altwegg, K., Berthelier, J.-J., et al. 2016, MNRAS, 462, S491
Haser, L. 1957, Bull. Soc. R. Sci. Liege, 43, 740
Heritier, K. L., Galand, M., Henri, P., et al. 2018, A&A, 618, A77
Johansson, F. L., Odelstad, E., Paulsson, J. J. P., et al. 2017, MNRAS, 469, S626
Johansson, F. L., Eriksson, A. I., Vigren, E., et al. 2021, A&A, 653, A128
Läuter, M., Kramer, T., Rubin, M., & Altwegg, K. 2018, MNRAS, 483, 852
Levasseur-Regourd, A. C., Mcbride, N., Hadamcik, E., & Fulle, M. 1999, A&A, 348, 636
Nilsson, H., Williamson, H., Bergman, S., et al. 2020, MNRAS, 498, 5263
Rubin, M., Koenders, C., Altwegg, K., et al. 2014, Icarus, 242, 38
Simon Wedlund, C., Behar, E., Nilsson, H., et al. 2020, A&A, 640, C3
Trotignon, J. G., Michau, J. L., Lagoutte, D., et al. 2007, Space Sci. Rev., 128, 713
Vigren, E., Galand, M., Eriksson, A. I., et al. 2015, ApJ, 812, 9
Vigren, E., Galand, M., Wellbrock, A., et al. 2016, ApJ, 826, 131
Vigren, E., Eriksson, A. I., Johansson, F. L., et al. 2021, Planet. Sci. J., 2, 156
Vigren, E., Eriksson, A. I., & Bergman, S. 2022, MNRAS, 513, 536